Icarus 203 (2009) 516–530

Contents lists available at ScienceDirect

Icarus

journal homepage: www.elsevier.com/locate/icarus

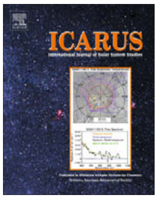

The jovian anticyclone BA
III. Aerosol properties and color change

S. Pérez-Hoyos [a,*], A. Sánchez-Lavega [a], R. Hueso [a], E. García-Melendo [b], J. Legarreta [c]

[a] *Grupo de Ciencias Planetarias, Dpto. Física Aplicada I, E.T.S. Ingeniería, Universidad del País Vasco, Bilbao, Spain*
[b] *Esteve Duran Observatory Foundation, Seva, Spain*
[c] *Departamento de Ingeniería de Sistemas y Automática, E.U.I.T.I., Universidad del País Vasco, Bilbao, Spain*

ARTICLE INFO

Article history:
Received 16 December 2008
Revised 26 June 2009
Accepted 30 June 2009
Available online 4 July 2009

Keywords:
Jupiter, Atmosphere
Atmospheres, Dynamics
Radiative transfer

ABSTRACT

A study of the vertical cloud structure of oval BA and its red color change is presented in this third part of our complete analysis. A large interest in Jupiter's anticyclone BA was created by its reddening that occurred between 2005 and 2006. In this work we quantify the color change in oval BA by using images taken with the Advanced Camera for Surveys (ACS) onboard the Hubble Space Telescope (HST) in six filters from the near ultraviolet (F250W) to the deep methane band in the near infrared (F892N). Reflectivity changes are noteworthy in nadir viewing geometry at the ultraviolet and blue wavelengths (F250W, F330W and F435W filters) but almost undetectable or inside error bars in the rest of filters (F550M, F658N and F892N). The observed reflectivity variations are discussed in terms of a commonly accepted vertical cloud structure model for jovian anticyclones in order to explore some causes for the color alteration. Our models of the observed reflectivity variation show that the vortex clouds did not change its vertical extension (top pressure) or its optical depth. We find that a change occurred in the absorbing properties of the particles populating the upper aerosols (single scattering albedo and imaginary refractive index). A discussion on the thermo-physical and dynamical properties of the vortex that could be in the origin of the color change is also presented.

1. Introduction

In the preceding parts I (García-Melendo et al., 2009) and II (Hueso et al., 2009) the detailed dynamical evolution of the oval BA since its formation in 2000 to the recent times has been addressed. This third part focuses on the vertical cloud structure and particle's optical properties at BA cloud tops, before and after the color change. We also address some dynamical scenarios that may intervene in the red coloration or in the spreading of a colorant throughout the vortex.

The vertical cloud structure of Jupiter's atmosphere has been studied in almost all the spectral ranges and following a number of techniques. Up to date, we have a relatively global knowledge of its main properties (e.g., see West et al., 1986, 2004 and references therein for the commonly accepted picture) although important features remain unclear (e.g. particles shapes, colorant agents, spatial and temporal scales for color variations, among others).

One of the most intriguing questions is the nature and behavior of the chromophore species that gives Jupiter's atmosphere its characteristic coloration and makes some regions redder than others. This agent is supposed to be ubiquitous and located at tropospheric levels (Simon-Miller et al., 2001b) but because of local concentrations of chemicals agents of unknown origin, some regions of the planet look redder than others (Simon-Miller et al., 2001a). West et al. (2004) presents a list of candidate chemical compounds that have been thought to be responsible for the coloration. At this moment, the correlation of the red colorant with the local dynamics, if any, is also unclear, so any clue to link a color change with a dynamical state (or change of it) would be a fundamental milestone in the understanding of Jupiter's physical and chemical atmospheric properties.

The first report of the oval BA reddening was made by amateur astronomers (Naeye, 2006) and Hubble Space Telescope observations with the Advanced Camera for Surveys (ACS) were later reported (Simon-Miller et al., 2006b). This work performed a principal component analysis of observations at different filters and stated that the main variation between 2005 and 2006 observations was related to the colorant agent in the blue wavelengths. A subsequent analysis of the oval BA (more closely related to the dynamical aspects) was presented by Cheng et al. (2008). The preceding papers I and II (García-Melendo et al., 2009; Hueso et al., 2009) showed a detailed analysis of the evolution and dynamical state of oval BA.

---

* Corresponding author. Address: Departamento Física Aplicada I, Escuela Técnica Superior de Ingeniería, Universidad del País Vasco, Alda. Urquijo s/n, 48013 Bilbao, Spain. Fax: +34 94 601 41 78.
E-mail address: santiago.perez@ehu.es (S. Pérez-Hoyos).

0019-1035/$ - see front matter © 2009 Elsevier Inc. All rights reserved.
doi:10.1016/j.icarus.2009.06.024

In this work, we provide the color change quantification in nadir viewing geometry from 2005 to 2006 HST ACS observations and present a vertical cloud structure modeling in order to compute how such a color change is related to atmospheric parameters. Section 2 shows the calibration process of the images and their result in terms of the reflectivity at the available filters. In Section 3 we model the observed reflectivity and determine the general vertical cloud structure and its spatial and temporal variations. A discussion on the physical scenarios that may be responsible in the oval history, according to results from the preceding parts I and II, is presented in Section 4.

2. Observations and photometric calibration

2.1. Description of the observations

We have used images obtained with the Advanced Camera for Surveys (ACS) onboard the Hubble Space Telescope (HST). This camera provides an outstanding spatial resolution together with good wavelength coverage. Since the color change was reported to happen during 2006, Jupiter observations from E. Karkoschka (January 2005, before the color change) and A. Simon-Miller and I. de Pater (April 2006, after the change) were used in order to quantify such color change. These archived data sets were retrieved from the HST Science Data Archive.

We selected a sub-set of filters simultaneously present in all the observational runs that covered the range from the ultraviolet (F250W) to the near infrared, including the deep methane band at 890 nm (F892N). Filters in the ultraviolet to blue wavelengths are wide (F250W, F330W, F435W) with full width half maximum of about 100 nm. Red filters (F658N and F892N) were narrow instead (FWHM of a few nanometers) so it is possible to constrain the effective methane absorption coefficient. Those coefficients were calculated by convolution of the filter response (Boffi et al., 2007) with the methane absorption spectrum (Karkoschka, 1998). An intermediate width filter at visible wavelengths was also used (F550M).

One of the problems with these observations is that they do not capture the oval BA at very different positions in the disk. Ideally, one would like to observe the oval from one limb to the next (i.e. spanning 180° longitude) but this is not possible in this case, with the images being separated typically by 20° longitude. This limits the information we can retrieve from the vertical cloud structure modeling although we can still compare the brightness of the oval at each wavelength in the two consecutive years in nadir viewing geometry. A summary of the selected images is presented in Table 1 and the resulting images of the oval BA are shown in Fig. 1.

Images were pipeline pre-processed and corrected from geometrical distortion and then navigated using LAIA software (see e.g. Sánchez-Lavega et al., 2001) in order to correlate pixel position with geometrical coordinates (latitude and longitude). After navigation, a planisphere or cylindrical projection was constructed with an under-sampled resolution of 0.5°/pixel.

2.2. Photometric calibration

Images were photometrically calibrated following the general specifications by the ACS team (Boffi et al., 2007) and, in particular, following the method explained by Li et al. (2006). The North–South average scans at the central meridian retrieved are compared in Fig. 2 with previous results by Chanover et al. (1995) finding a good agreement between both set of results in all filters. Some ACS images provide information on more northern latitudes but in this figure we are limited to the most restricting observations.

The same procedure was applied to the 2006 observations. However, some individual images were about a 15% brighter or darker than 2005 and reference photometry. Those image results were corrected by reference to the meridional profiles. Fig. 2 also shows that the expected dispersion at a given location (i.e. not affecting simultaneously to the whole meridional profile) can amount up to a 10% of the observed reflectivity.

Table 1
Summary of the observations.

Image	Filter	Date
j90502nlq	F330W	*HST ACS*
j90502nmq	F435W	19/01/2005
j90502nnq	F658N	Karkoschka
j90502noq	F892N	
j90502npq	F250W	
j90502nsq	F330W	
j90502ntq	F435W	
j90502nuq	F658N	
j90502nvq	F892N	
j90502nwq	F250W	
j90502nxq	F330W	
j90502nyq	F435W	
j90502nzq	F658N	
j90502o0q	F892N	
j90502o1q	F250W	
j90502o2q	F330W	
j90502o3q	F435W	
j90502o4q	F550M	
j90502o5q	F658N	
j90502o6q	F892N	
j9mj01ivq	F892N	*HST ACS*
j9mj01iuq	F658N	08/04/2006
j9mj01itq	F550M	Simon-Miller
j9mj01ipq	F435W	
j9mj01inq	F330W	
j9mj01imq	F250W	
j9mj01ikq	F658N	
j9mj01ijq	F435W	
j9mj01iiq	F550M	
j9mj01ihq	F892N	
j9mj01igq	F658N	
j9mj01ifq	F550M	
j9mj01ibq	F435W	
j9mj01iaq	F330W	
j9mj01i9q	F250W	
j9mm06esq	F892N	*HST ACS*
j9mm06elq	F658N	24/04/2006
j9mm06ekq	F435W	de Pater
j9mm06eoq	F658N	
j9mm04c4q	F658N	
j9mm04c7q	F658N	
j9mm04c6q	F435W	
j9mm04buq	F550M	
j9mm04btq	F330W	
j9mm04bsq	F892N	
j9mm04bxq	F550M	
j9mm04bpq	F658N	
j9mm04bwq	F330W	
j9mm04bvq	F892N	
j9mm04bnq	F435W	
j9mm04bmq	F658N	

2.3. The limb darkening behavior of the oval

Before we quantify the color change in the oval we summarize the limb darkening information. Since we will later reduce observational data to an idealized nadir viewing geometry, we need to take care of how the oval observed reflectivity is affected by its position in the planetary disk with respect to the central meridian. For doing so, we use an empirical Minnaert's law defined as follows (Minnaert, 1941):

$$I/F = (I/F)_0 \mu_0^k \mu^{k-1} \tag{1}$$

Here I/F is the observed reflectivity, $(I/F)_0$ the geometrically corrected reflectivity, μ and μ_0 the cosines of the observing and